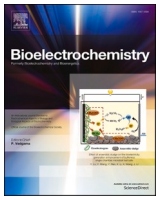
Bioelectrochemistry 165 (2025) 108975



Contents lists available at ScienceDirect

Bioelectrochemistry

journal homepage: www.journals.elsevier.com/bioelectrochemistry



Hybridization chain reaction and CRISPR/Cas12a-integrated biosensor for precise Ago2 detection

Qiang Tang [a], Jiayi Zhang [b], Jialuo Pang [a], Yingying Huang [a], Ying Guan [a], Yuanxun Gong [a], Qianli Tang [a,*], Kai Zhang [c,*], Xianjiu Liao [b,*]

[a] Guangxi Key Laboratory for Preclinical and Translational Research on Bone and Joint Degenerative Diseases, Affiliated Hospital of Youjiang Medical University for Nationalities, Baise, Guangxi, 533000, China
[b] West Guangxi Key Laboratory for Prevention and Treatment of High-incidence Diseases, Youjiang Medical University for Nationalities, Baise, Guangxi, 533000, China
[c] School of Chemistry and Materials Science, Nanjing University of Information Science and Technology. Nanjing, 210044, China

ARTICLE INFO

Keywords:
Electrochemiluminescence (ECL) biosensor
Hybridization chain reaction (HCR)
CRISPR/Cas12a system
Argonaute 2 (Ago2) detection
Signal amplification

ABSTRACT

This study introduces an innovative electrochemiluminescence (ECL) biosensor for the highly sensitive and specific detection of Argonaute 2 (Ago2) activity. Ago2, a key enzyme in the RNA interference (RNAi) pathway, plays a crucial role in gene regulation, and its dysregulation is associated with diseases such as cancer and viral infections. The biosensor integrates hybridization chain reaction (HCR) amplification and the CRISPR/Cas12a system, leveraging a multi-stage signal amplification strategy. The detection mechanism begins with Ago2-mediated cleavage of a designed hairpin RNA (HP-RNA), releasing single-stranded RNA (ssRNA) that triggers HCR. This amplification step generates long DNA polymers, which serve as activators for the CRISPR/Cas12a system. Cas12a's collateral cleavage activity amplifies the signal further by cleaving a DNA reporter labeled with a ruthenium-based luminophore, enhancing the ECL output. This dual amplification strategy achieves exceptional sensitivity, with a detection limit of 0.126 aM. The biosensor demonstrates excellent specificity, distinguishing Ago2 from other Argonaute proteins, and maintains high reproducibility and stability, retaining 94 % of its signal after two weeks of storage. Real-world applicability was confirmed by accurately detecting Ago2 in spiked cell lysates, with recovery rates exceeding 100 %. The combination of HCR, CRISPR/Cas12a, and ECL establishes a robust platform for biomarker detection, offering superior sensitivity and adaptability for clinical diagnostics, disease monitoring, and therapeutic evaluation. This biosensor represents a significant advancement in the development of next-generation diagnostic tools.

1. Introduction

Argonaute 2 (Ago2) is a pivotal enzyme in the RNA interference (RNAi) pathway, a fundamental mechanism for regulating gene expression at the post-transcriptional level [1–3]. It plays a central role in the RNA-induced silencing complex (RISC), which mediates the cleavage of target messenger RNA (mRNA) in response to small regulatory RNAs, such as microRNAs (miRNAs) and small interfering RNAs (siRNAs) [4,5]. This process is essential for controlling various physiological functions, including cellular differentiation, proliferation, immune responses, and stress adaptation. Dysregulated Ago2 activity, either upregulation or downregulation, has been associated with numerous pathological conditions such as cancer, viral infections, and neurodegenerative diseases [5–7]. For example, overexpression of Ago2 has been linked to enhanced proliferation and invasiveness of cancer cells, making it a crucial biomarker for early disease detection and prognosis. Therefore, precise and sensitive monitoring of Ago2 activity is not only vital for understanding the mechanistic underpinnings of gene silencing but also holds promise for the development of diagnostic tools, therapeutic interventions, and personalized treatment strategies [8–10].

To achieve sensitive detection of nucleic acid targets, various amplification techniques have been explored. Among these, the hybridization chain reaction (HCR) has emerged as a promising non-enzymatic amplification strategy [11,12]. HCR is an isothermal reaction in which a target nucleic acid triggers a cascade of hybridization events, leading to the formation of a long double-stranded DNA polymer [13]. Compared to conventional enzymatic amplification methods such

* Corresponding authors.
E-mail addresses: htmgx919@163.com (Q. Tang), kaizhang@nuist.edu.cn (K. Zhang), lxj2009919@163.com (X. Liao).

https://doi.org/10.1016/j.bioelechem.2025.108975
Received 17 February 2025; Received in revised form 7 March 2025; Accepted 18 March 2025
Available online 26 March 2025
1567-5394/© 2025 Published by Elsevier B.V.

as polymerase chain reaction (PCR) or loop-mediated isothermal amplification (LAMP), HCR offers several distinct advantages [14–16]. Firstly, it is an enzyme-free amplification process, which significantly reduces the risk of contamination and the need for strict temperature control, thus making it more suitable for point-of-care and on-site applications [12,17,18]. Secondly, HCR's simplicity in operation, along with its ability to generate long DNA polymers that can serve as scaffolds for further amplification steps, enhances its utility in biosensing applications [19,20]. Moreover, HCR is highly programmable, allowing for customization of the target recognition sequence, which adds flexibility in designing assays for different biomarkers. Given these advantages, HCR is an excellent candidate for integration into a multi-stage amplification system to enhance the sensitivity and specificity of biosensors.

CRISPR/Cas systems, originally discovered as an adaptive immune system in bacteria and archaea, have revolutionized the field of molecular diagnostics [21–26]. The CRISPR/Cas12a system, in particular, has gained significant attention due to its collateral cleavage activity [27–29]. Upon recognition and binding of a target DNA sequence by the CRISPR RNA (crRNA)-guided Cas12a enzyme, the activated Cas12a exhibits nonspecific single-stranded DNA (ssDNA) cleavage activity, which can be exploited for signal amplification [30–32]. This collateral cleavage property makes Cas12a highly suitable for developing biosensors with low detection limits [33,34]. CRISPR/Cas12a-based biosensors exhibit several advantages, including high specificity due to the sequence-dependent recognition of the target by crRNA, and high sensitivity through collateral cleavage that leads to amplification of the detection signal [35,36]. Additionally, the programmability of the CRISPR/Cas12a system allows for easy adaptation to detect various nucleic acid targets by simply changing the crRNA sequence, thus providing a versatile platform for the detection of different biomarkers. The integration of CRISPR/Cas12a into biosensing systems has already shown great potential in detecting pathogens, cancer biomarkers, and other clinically relevant targets [31,37].

In this study, we designed an electrochemiluminescence (ECL) biosensor [38] for the sensitive detection of Ago2 activity, integrating HCR amplification and the CRISPR/Cas12a system. The detection strategy is as follows: Ago2 specifically cleaves a designed hairpin RNA substrate, releasing a single-stranded RNA product. This product then serves as the initiator for the HCR, wherein two complementary DNA hairpins (HP1 and HP2) undergo sequential hybridization to form a long double-stranded DNA polymer. The HCR product contains protospacer adjacent motif (PAM) sequences and protospacer regions, which can be specifically recognized by the Cas12a/crRNA complex. Upon binding of the Cas12a/crRNA complex to the HCR product, the collateral cleavage activity of Cas12a is activated, leading to the cleavage of a single-stranded DNA reporter that is directly linked to changes in the electrochemiluminescence signal. The cleavage of this reporter molecule ultimately generates an amplified ECL signal that can be quantitatively measured.

The integration of HCR and CRISPR/Cas12a in this biosensor design provides multiple layers of amplification. The initial cleavage of the hairpin RNA by Ago2 ensures that only active Ago2 can trigger the downstream processes, thereby enhancing the specificity of the detection. The HCR amplification step converts each RNA cleavage event into multiple DNA duplexes, significantly increasing the amount of target available for subsequent detection. Finally, the collateral cleavage activity of Cas12a provides further signal amplification by cleaving multiple ssDNA reporters for each target molecule recognized, thereby triggering a significant change in the ECL signal output. The use of electrochemiluminescence as the signal output further enhances the sensitivity of the biosensor, due to the low background noise and high signal-to-noise ratio characteristic of ECL detection. This multi-stage amplification strategy enables highly sensitive detection of Ago2 activity, with potential applications in early diagnosis, therapeutic monitoring, and personalized medicine for diseases where Ago2 plays a critical role.

2. Materials and method

2.1. Materials and chemical reagents

All oligonucleotides, including hairpin RNA substrates, HCR hairpins (HP1, HP2 and HP3), and single-stranded DNA reporters (DNA1), were synthesized by Sangon Biotech (Shanghai, China) (Table S1). The hybridization buffer for HCR contained 20 mM Tris-HCl (pH 7.5), 140 mM NaCl, and 5 mM KCl. Electrochemiluminescence (ECL) was performed using $[Ru(bpy)_3]Cl_2$ (Sigma-Aldrich, USA) as the luminophore, with tri-n-propylamine (TPrA, Aladdin, China) as the co-reactant. The human Ago2 protein was purchased from Sino Biological (Beijing, China). All reagents were of analytical grade, and DEPC-treated ultrapure water was used to prevent RNase contamination.

2.2. Preparation of $Ru(bpy)_3^{2+}$-NHS and Probe Labeling Procedure

Following established protocols, we synthesized the $Ru(bpy)_3^{2+}$-NHS complex for probe labeling. First, $Ru(bpy)_2(dcbpy)(PF_6)_2$ was prepared by refluxing $Ru(bpy)_2Cl_2$ with excess dcbpy (4,4′-dicarboxylic acid-2,2′-bipyridine). $NaPF_6$ was added to convert it to a stable PF_6 salt, improving its solubility.

Next, $Ru(bpy)_2(dcbpy)(PF_6)_2$ was activated by treating with N-hydroxysuccinimide (NHS) and dicyclohexylcarbodiimide (DCC) in DMF, forming the $Ru(bpy)_3^{2+}$-NHS ester for labeling the amino-modified DNA sequence. The conjugation was achieved by reacting the NHS ester with the DNA in a sodium borate buffer (pH 8.5) at a 30:1 M ratio. The product was purified by ethanol washing and centrifugation to remove unreacted materials, and the $Ru(bpy)_3^{2+}$-conjugated probes (DNA1–Ru) were stored at 4 °C for stability. These conjugates are suitable for biosensor and molecular detection assays, utilizing their electrochemiluminescent properties for sensitive analysis.

2.3. Ago2 cleavage HP-RNA

To prepare the reaction mixture, we began by combining 200 nM guide RNA (gRNA), 600 nM blocker RNA, and 1× Ago2 reaction buffer, which contained 30 mM Tris (pH 7.5), 130 mM KCl, 1.1 mM $MgCl_2$, 1 mM DTT, and 0.1 mM EDTA, in a total reaction volume of 50 μL. This Ago2 reaction buffer was specifically chosen to optimize Ago2 activity by providing the necessary ionic conditions for the RNA cleavage reaction and maintaining enzyme stability. The mixture was incubated at 30 °C for 30 min to allow Ago2 to interact with the guide RNA and HP-RNA, initiating the RNA silencing process. Varying concentrations of Ago2 were tested to evaluate its impact on the reaction efficiency and the subsequent signal amplification, offering insights into the enzyme's role in modulating the biosensor response.

2.4. HCR Reaction

The hybridization chain reaction (HCR) is a non-enzymatic amplification technique in which two or more complementary hairpin DNA sequences interact with a target nucleic acid, leading to the formation of long double-stranded DNA polymers. In this study, HP1, HP2, and HP3 hairpins, each at a concentration of 1 μM, were annealed separately to ensure proper folding into stable hairpin structures. The annealing process was performed in a buffer containing 20 mM Tris-HCl (pH 7.5), 140 mM NaCl, and 5 mM KCl, which provides optimal ionic conditions for stabilizing DNA secondary structures. The annealing was conducted using a PCR thermocycler under the following thermal protocol: heating at 95 °C for 5 min to denature any undesired secondary structures, followed by gradual cooling to Tm-5 °C for 30 min to facilitate specific annealing, then holding at 37 °C for 30 min to maintain stable hairpin formation, and finally cooling to 4 °C for 30 min to ensure complete stabilization of the hairpins.

The HCR reaction was initiated by mixing the three hairpins, HP1,

HP2, and HP3, with the target part of HP-RNA in a 10 μL reaction volume. The reaction mixture contained 300 nM HP1, 500 nM HP2, and 500 nM HP3, along with varying concentrations of the target part of HP-RNA. The reaction was conducted at 37 °C for 30 min to allow the target part of HP-RNA to trigger the opening of the HP1 hairpin. Upon recognition of the target part of HP-RNA, HP1 undergoes conformational changes, exposing a sticky end that hybridizes with HP2, which, in turn, triggers the unfolding of HP2 and subsequent binding to HP3. This cascade process continues, forming extended DNA duplexes composed of alternating HP2 and HP3 units.

The concentrations of HP1, HP2, and HP3 were carefully optimized to ensure efficient amplification while minimizing non-specific interactions that could lead to background noise. Specifically, HP1 was set at a lower concentration (300 nM) compared to HP2 and HP3 (500 nM each), ensuring that HP1 primarily functions as the initiator, facilitating controlled hybridization and avoiding excessive non-specific interactions. The higher concentrations of HP2 and HP3 promote the propagation of the chain reaction, enhancing the efficiency of amplification and ensuring that the process continues without premature termination.

This careful optimization of hairpin concentrations balances the need for effective amplification with the goal of minimizing background signals. The reaction conditions, including 37 °C for 30 min, were chosen to allow sufficient amplification while keeping the background noise minimal, ensuring that the system is highly sensitive without generating significant non-specific signals. The resulting HCR product, consisting of long nicked double-stranded DNA polymers, serves as an activator for downstream processes such as CRISPR/Cas12a-based collateral cleavage, further enhancing the overall detection sensitivity of the biosensor.

2.5. CRISPR Cas12a activation and ECL measurement

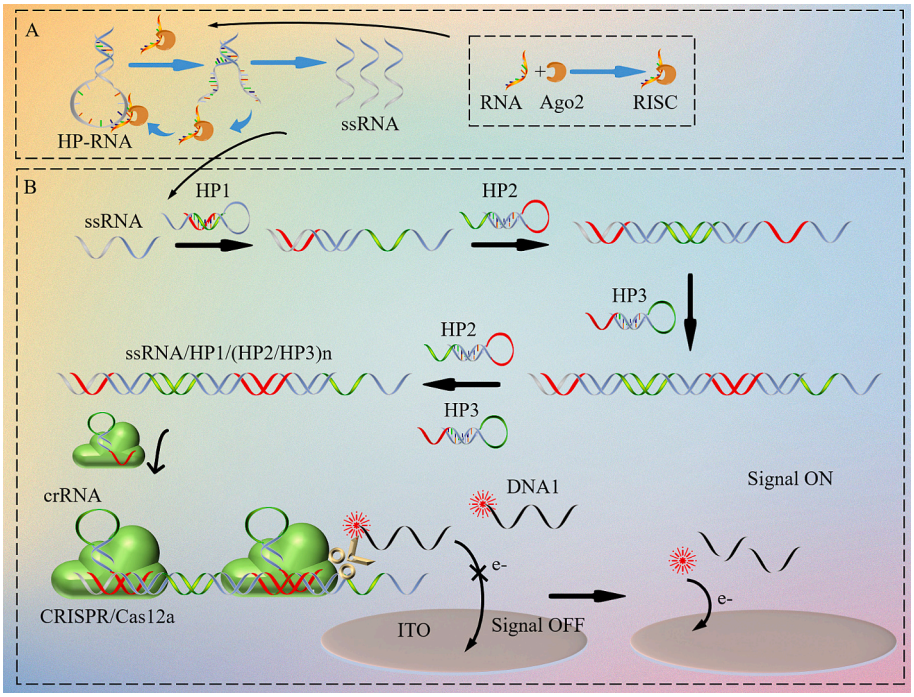
To prepare the Cas12a/crRNA ribonucleoprotein (RNP) complex, Cas12a (100 nM) was incubated with crRNA (100 nM) at 37 °C for 10 min in 1× NEBuffer 2.1. This incubation allows the formation of an active ribonucleoprotein complex capable of recognizing and cleaving target DNA sequences. Following the formation of the Cas12a/crRNA complex, 20 μL of HCR product and 10 μL of ECL reporter (20 μM) were added to the pre-assembled complex, and the final reaction volume was adjusted to 200 μL. The complete reaction mixture was then incubated in a microcentrifuge tube at 37 °C for 20 min, with electrochemiluminescence (ECL) measurements taken.

3. Results and discussion

3.1. The working principle

The proposed biosensor for detecting Ago2 activity integrates a multi-stage amplification strategy involving a hybridization chain reaction (HCR), CRISPR/Cas12a, and electrochemiluminescence (ECL) as the signal readout (See Scheme 1A and B). This novel design leverages the specificity of Ago2-mediated cleavage, the amplification capability of HCR, and the sensitive detection afforded by Cas12a collateral cleavage to provide a highly sensitive and specific detection platform.

The detection process begins with the formation of the RNA-Induced Silencing Complex (RISC), as illustrated in Scheme 1A. Ago2, a core component of RISC, recognizes and binds to a specifically designed hairpin RNA (HP-RNA). This HP-RNA contains a sequence that is targeted exclusively by Ago2, ensuring that only active Ago2 can trigger the subsequent reaction. Upon binding, Ago2 cleaves the HP-RNA, resulting in the release of a single-stranded RNA product (ssRNA).



Scheme 1. Schematic Illustration of the Biosensor Detection Mechanism. (A) Ago2 Recognition and Cleavage Step: Ago2, a key enzyme in the RNA-Induced Silencing Complex (RISC), specifically recognizes and cleaves the designed hairpin RNA (HP-RNA), resulting in the release of single-stranded RNA (ssRNA). This ssRNA serves as the initiator for the subsequent hybridization chain reaction (HCR)-driven amplification process. (B) Multi-Stage Signal Amplification via HCR and CRISPR/Cas12a: The released ssRNA initiates a cascading HCR, triggering a stepwise hybridization reaction among hairpins HP1, HP2, and HP3 to form an extended double-stranded DNA polymer. This amplified DNA product is subsequently recognized by CRISPR/Cas12a, which, upon activation, exhibits collateral cleavage activity. Cas12a indiscriminately cleaves $Ru(bpy)_3^{2+}$-tagged DNA reporter sequences, producing fragmented DNA with reduced electrostatic repulsion. These fragments diffuse more efficiently toward the indium tin oxide (ITO) electrode surface, enhancing electron transfer efficiency and significantly boosting the electrochemiluminescence (ECL) signal, enabling ultrasensitive detection of Ago2 activity.

This ssRNA is crucial, as it serves as the initiator for the downstream amplification processes, providing an initial layer of specificity where only the correct target generates the necessary RNA product for further reactions.

The released single-stranded RNA (ssRNA) acts as the initiator for the hybridization chain reaction (HCR), as shown in Scheme 1B. In this HCR process, three complementary DNA hairpins—HP1, HP2, and HP3—are utilized. The initiator ssRNA binds to HP1, causing the opening of its hairpin structure and exposing a sticky end that is complementary to HP2. This triggers a cascading reaction where HP2 unfolds and hybridizes with HP3, which then further hybridizes with HP1, resulting in the formation of a long, extended double-stranded DNA polymer composed of alternating HP1, HP2, and HP3 units. This amplification cycle significantly enhances the initial signal, allowing the generation of a large quantity of double-stranded DNA polymers from a single cleavage event. HCR, as a non-enzymatic amplification process, operates under isothermal conditions, which makes it easy to execute and ensures a high level of sensitivity.

The amplified HCR product contains specific sequences that are recognized by the CRISPR/Cas12a system. Cas12a, guided by a CRISPR RNA (crRNA) that is complementary to a target sequence within the HCR product, binds to the amplified product and becomes activated. Upon activation, Cas12a exhibits collateral cleavage activity, which allows it to cleave not only the target sequence but also other nearby single-stranded DNA molecules nonspecifically. In this biosensor design, the target for Cas12a's collateral cleavage is a DNA reporter sequence tagged with $Ru(bpy)_3^{2+}$, a ruthenium-based luminophore utilized for generating an ECL signal.

Upon cleavage of the $Ru(bpy)_3^{2+}$-tagged DNA1 reporter by activated Cas12a, the DNA is fragmented into shorter pieces, effectively reducing the overall negative charge density on the reporter fragments. This reduction in charge minimizes electrostatic repulsion between the negatively charged DNA fragments and the indium tin oxide (ITO) electrode surface, allowing for their closer diffusion toward the electrode.

As these $Ru(bpy)_3^{2+}$-tagged fragments accumulate near the ITO electrode, the proximity enhances electron transfer efficiency, leading to a significant boost in the ECL signal intensity. Additionally, the collateral cleavage activity of Cas12a ensures continuous fragmentation of the DNA reporters, further amplifying the signal output. This multi-step amplification mechanism, which integrates enzymatic cleavage, electrostatic modulation, and enhanced electrode interaction, establishes a highly sensitive and specific detection system. The synergistic effects of these processes enable the biosensor to achieve ultrasensitive Ago2 detection with exceptional precision, setting it apart from conventional ECL-based detection platforms.

The ECL signal generated by the $Ru(bpy)_3^{2+}$-tagged fragments is monitored in real-time, providing quantitative data on Ago2 activity. The use of ECL as the readout provides several advantages: it offers high sensitivity due to efficient light emission from the $Ru(bpy)_3^{2+}$ complex when electrochemically excited, has low background noise for precise detection, and allows for continuous monitoring of reaction kinetics to understand the dynamics of Ago2 activity in detail.

By measuring the rate of ECL intensity increase over time, the biosensor is capable of quantitatively determining Ago2 concentration. The integration of HCR for nucleic acid amplification and CRISPR/Cas12a for enzymatic amplification ensures that the biosensor achieves an extremely sensitive detection limit. This multi-layered approach makes it an ideal tool for applications in clinical diagnostics, disease monitoring, and therapeutic evaluation.

3.2. Feasibility of experimental conditions

Electrochemiluminescence (ECL) measurements were conducted to evaluate the efficiency of the newly developed homogeneous ECL biosensor for Ago2 detection, as shown in Fig. 1A. Initially, the ECL signal was minimal (curve a) when only the probe DNA1 was present, suggesting significant electrostatic repulsion that hindered the $Ru(bpy)_3^{2+}$-tagged probe from reaching the ITO electrode surface. This initial weak signal demonstrated the challenges posed by the electrostatic interactions between the negatively charged DNA probe and the electrode surface, which limited the efficient approach of the labeled probe molecules [39].

Following the implementation of the dual amplification strategy and enzymatic cleavage by CRISPR/Cas12a (at 10000 aM Ago2), a substantial increase in ECL signal was observed (curve b). This

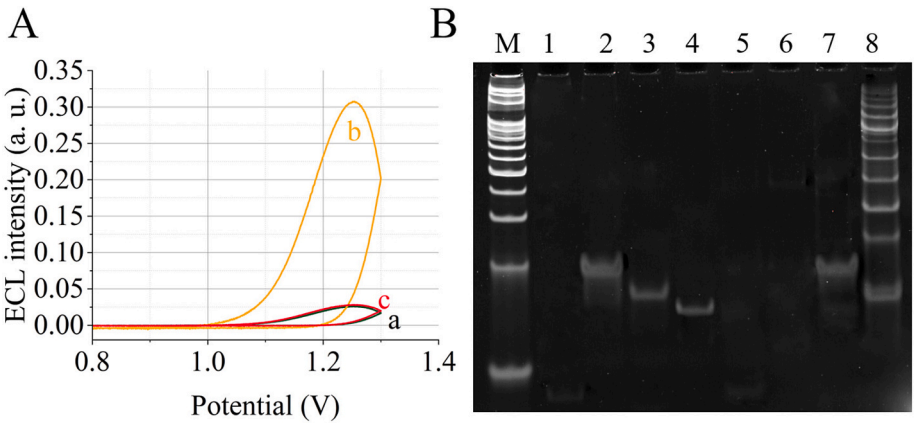


Fig. 1. (A) ECL signal profiles for evaluating the feasibility of the homogeneous ECL biosensor under experimental conditions. (a) Minimal ECL signal observed when only probe DNA1 was present, indicating significant electrostatic repulsion between the $Ru(bpy)_3^{2+}$-tagged probe and the negatively charged electrode surface. (b) Substantial increase in ECL signal after the application of the dual amplification strategy and CRISPR/Cas12a-mediated enzymatic cleavage at 10,000 aM Ago2. The cleavage of DNA1 into shorter fragments led to reduced electrostatic barriers, enabling enhanced proximity of $Ru(bpy)_3^{2+}$-tagged fragments to the electrode surface and resulting in improved ECL intensity. The combined effects of RISC-assisted signal amplification and CRISPR/Cas12a collateral cleavage contributed to the high sensitivity of the biosensor for low-abundance target detection. (c) HP1-treated Cas12a with electrode-modified DNA. No notable signal change when HP1-treated Cas12a was used, confirming that HP1 alone does not activate Cas12a, preventing false-positive signals. (B) Polyacrylamide gel electrophoresis (PAGE) Analysis of HCR Initiation: PAGE analysis confirming the successful initiation of the hybridization chain reaction (HCR) by single-stranded RNA (ssRNA). Lane M: Molecular weight marker; Lane 1: ssRNA alone; Lane 2: Hairpin H1; Lane 3: Hairpin H2; Lane 4: Hairpin H3; Lane 5: H1 + ssRNA; Lane 6: H1 + H2 + ssRNA; Lane 7: H1 + H2 + H3 (without ssRNA); Lane 8: H1 + H2 + H3 + ssRNA. The appearance of new bands in Lane 8, corresponding to HCR products, and the reduction or absence of individual bands for ssRNA and hairpins confirm efficient HCR initiation. The absence of additional bands in Lane 7 indicates that the hairpins remain stable without ssRNA, demonstrating minimal background interference.

enhancement is attributed to the enzymatic cleavage of the DNA1 probe into shorter fragments, which, due to their lower charge, were able to overcome electrostatic barriers more effectively, facilitating closer proximity of the $Ru(bpy)_3^{2+}$-tagged fragments to the ITO electrode. The reduction in fragment size and charge density significantly improved their ability to diffuse toward the electrode, leading to a more efficient electron transfer and thus enhancing the ECL response.

This enhanced proximity led to a significant boost in the ECL signal, demonstrating the effectiveness of the combined amplification mechanisms. The overall improvement was achieved through the combined effects of RNA-induced silencing complex (RISC)-assisted signal amplification and CRISPR/Cas12a enzymatic activity, which together facilitated multiple stages of signal amplification. The RISC complex, by assisting in the initial cleavage, allowed for the precise generation of target fragments, while CRISPR/Cas12a further amplified the signal through its collateral cleavage activity. These complementary processes ensured a highly amplified and easily detectable ECL response, making the biosensor suitable for low-abundance target detection.

Additionally, to address concerns regarding the potential activation of Cas12a by HP1 and the possibility of false-positive signals, we have conducted control experiments and analyzed the results presented in Fig. 1A. Specifically, curve c represents the ECL signal obtained when HP1-treated CRISPR/Cas12a was used to cleave the electrode surface-modified DNA. The results show that the ECL signal did not increase significantly, indicating that HP1 alone did not activate Cas12a's cleavage activity. This confirms that HP1 cannot independently trigger Cas12a-mediated collateral cleavage, thereby minimizing the risk of false-positive signals. These findings provide strong evidence that Cas12a activation in our biosensor strictly depends on the complete hybridization chain reaction (HCR) process and the presence of the specific target, ensuring high specificity in Ago2 detection.

As shown in Fig. 1B, the polyacrylamide gel electrophoresis (PAGE) results provide clear experimental evidence confirming the successful initiation of the hybridization chain reaction (HCR) by single-stranded RNA (ssRNA). Lane M represents the molecular weight marker, while Lane 1 contains the ssRNA alone, serving as a reference for its migration pattern. Lanes 2, 3, and 4 display the individual hairpin structures (H1, H2, and H3, respectively), each appearing as distinct bands, indicating their proper folding and stability.

Upon mixing the hairpins with ssRNA, distinct changes in band patterns are observed. Lane 5 (H1 + ssRNA) and Lane 6 (H1 + H2 + ssRNA) show partial hybridization, while Lane 7, which contains H1, H2, and H3 without ssRNA, exhibits no additional bands, confirming that the hairpins remain stable in the absence of an initiator. In Lane 8, where ssRNA, H1, H2, and H3 are combined, multiple new bands appear, corresponding to the hybridized HCR product. The reduction or disappearance of the individual bands for ssRNA and hairpins in this lane confirms that HCR proceeds efficiently upon ssRNA initiation. Furthermore, the absence of significant non-specific bands in Lane 7 highlights the system's stability and specificity, ensuring minimal background interference. These results are consistent with previous studies demonstrating that HCR can be precisely controlled by target ssRNA sequences, reinforcing the effectiveness of the designed biosensor strategy.

3.3. Optimization of the experimental conditions

As illustrated in Fig. 2A, the ECL signal showed a marked increase with the cleavage time of Ago2, ranging from 0 to 30 min. This gradual rise in signal intensity is indicative of the ongoing cleavage and subsequent amplification process, where more Ago2 leads to an increased generation of target fragments, further triggering the hybridization chain reaction (HCR). The signal eventually plateaued after 30 min, indicating that the reaction had reached its saturation point, and the optimal time for transcriptional amplification had been achieved. The saturation of the ECL signal suggests that the majority of the hairpin substrates had already participated in the amplification process, making 30 min the ideal duration for maximal efficiency.

Fig. 2B explores the effect of various durations of Cas12a-mediated cleavage on the ECL signal output. The results showed a notable increase in ECL intensity as the Cas12a reaction time was extended, highlighting the importance of allowing sufficient time for Cas12a's collateral cleavage activity to fully activate and cleave the $Ru(bpy)_3^{2+}$-tagged DNA1 reporter. The optimal duration for Cas12a activity was determined to be 30 min, as extending the cleavage beyond this time resulted in a negligible increase in ECL signal, indicating that the reaction had reached its maximum efficiency. This optimal timeframe allows for maximal target cleavage and effective signal amplification while avoiding unnecessary extension that may not contribute to further sensitivity gains.

The observed trends in both Ago2 and Cas12a cleavage times are critical for optimizing the overall performance of the biosensor. Ensuring that each component of the amplification strategy has sufficient time to complete its respective reaction steps is key to achieving a robust signal. The dual amplification approach, involving both HCR and Cas12a, relies heavily on the synchronization of these two processes, with the cleavage of the DNA1 probe by Ago2 setting the stage for subsequent HCR and Cas12a reactions. The plateau observed after 30 min for both processes underscores the efficiency of the system in reaching maximum signal amplification without excessive time

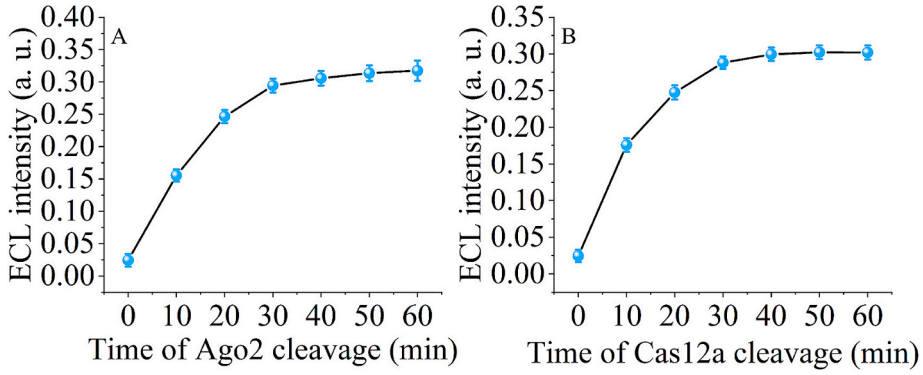


Fig. 2. Optimization of the experimental conditions for Ago2 and Cas12a cleavage. (A) ECL signal as a function of the cleavage time of Ago2, ranging from 0 to 60 min. The ECL intensity increased steadily up to 30 min, indicating efficient cleavage and subsequent hybridization chain reaction (HCR) amplification, before reaching a plateau, suggesting the optimal duration for Ago2 activity was 30 min. (B) Effect of Cas12a-mediated cleavage time on ECL signal output, with a similar trend observed. The ECL intensity increased significantly up to 30 min of incubation, after which it reached a maximum, suggesting 30 min as the optimal time for Cas12a activity. These results highlight the importance of synchronization between Ago2 cleavage and Cas12a collateral cleavage activity for achieving optimal biosensor performance, making 30 min the ideal duration for both reactions to ensure maximum signal amplification without unnecessary incubation time.

requirements, thereby making the biosensor suitable for rapid and sensitive detection applications.

3.4. ECL biosensor performance analysis

Electrochemiluminescence (ECL) biosensors are highly regarded for their remarkable sensitivity and specificity in biomolecule detection. In this study, we investigated the performance of an ECL biosensor specifically designed for Ago2 detection. The results demonstrated a substantial increase in ECL signal intensity corresponding to higher concentrations of Ago2, ranging from 5 attomolar (aM) to 10 femtomolar (fM), as depicted in Fig. 3. Notably, Fig. 3A illustrates the direct correlation between Ago2 concentration and the intensity of the ECL signal, with a peak observed around 10 fM. This peak suggests optimal enzymatic cleavage by the DNA1-Ru conjugate, which is crucial for maximizing signal generation.

Fig. 3B further provides a detailed examination of the relationship between the logarithmic values of Ago2 concentrations and the corresponding ECL intensities. The linearity of this relationship is described by the regression eq. $Y = -0.0629 + 0.0872\ \lg X$, with an R^2 value of 0.9990, indicating a strong correlation and confirming the precision of the biosensor in quantifying Ago2 levels across a broad concentration range.

The calculated limit of detection (LOD) for the biosensor, using the 3σ/slope method, was found to be 0.126 aM, reflecting its exceptional sensitivity. This LOD surpasses many currently available methods, as summarized in Table 1. In the LOD calculation, 'σ' represents the standard deviation obtained from blank assay measurements, while 'slope' denotes the gradient of the linear calibration curve. The outstanding sensitivity of this biosensor is primarily due to the dual signal amplification strategy employed: the initial signal amplification triggered by Ago2-mediated RNA cleavage and the precise enzymatic activity of CRISPR/Cas12a, which further amplifies the detection signal. (See Table 1.)

Compared to previous studies on Cas12a-based biosensors (Table 1), this work demonstrates a significantly improved detection limit (0.126 aM), which is orders of magnitude more sensitive than previously reported methods. The integration of hybridization chain reaction (HCR) and CRISPR/Cas12a-mediated collateral cleavage achieves a highly efficient dual amplification strategy, surpassing conventional single-step amplification approaches. Moreover, the use of electrochemiluminescence (ECL) enhances detection specificity and stability, providing a robust platform for highly sensitive Ago2 quantification. Unlike traditional strategies, which often suffer from limited sensitivity or complex operational procedures, this biosensor offers superior analytical performance, excellent reproducibility, and practical applicability for detecting Ago2 in biological samples. These advantages establish this work as a significant advancement in Cas12a-based biosensing, broadening its potential applications in clinical diagnostics and disease monitoring.

Table 1
Comparison of Detection Limits and Performance Characteristics of Various Ago2 Detection Methods.

Detection Method	Detection Strategy	Detection Limit	Reference
DNAzyme biosensor	Rolling circle amplification and DNAzyme-mediated dual signal amplification	0.35 pM	[40]
Gold nanoparticle-based single-molecule biosensor	Single-molecule counting of Cy5-labeled probes released from AuNPs	9.1 pM	[1]
DNA Tetrahedron Based Biosensor	Photoinduced electron-transfer (PET) fluorescence detection	4.54 nM	[41]
ECL biosensor (This work)	HCR + CRISPR/Cas12a-based dual signal amplification	0.126 aM	This work

Table 1
Determination of Ago2 in cell lysate by using the biosensor ($n = 3$). The cell lysate was diluted 10-fold by 0.01 M PBS.

Sample	Add (aM)	Found (aM)	Recovery (%)	RSD (%)
1	0	9.56	null	3.86
2	50	60.49	101.86	4.32
3	100	113.33	103.77	5.26
4	500	512.56	100.6	4.68
5	1000	1022.89	101.333	4.63

The dual amplification mechanism is integral to the system's effectiveness, with each amplification step contributing significantly to the overall sensitivity. First, Ago2-mediated cleavage generates an RNA product that triggers HCR (Hybridization Chain Reaction). This initial amplification step creates a significantly amplified DNA signal, which is essential for increasing the target concentration and providing a substrate for the next amplification stage. HCR serves as the first layer of amplification, producing long DNA polymers that substantially increase the amount of detectable signal, thus enhancing the biosensor's sensitivity.

The second amplification step involves Cas12a cleavage. Once activated by the HCR product, Cas12a introduces a further level of amplification through its collateral cleavage of the labeled DNA reporter. This step is highly efficient, as Cas12a cleaves multiple reporter molecules for

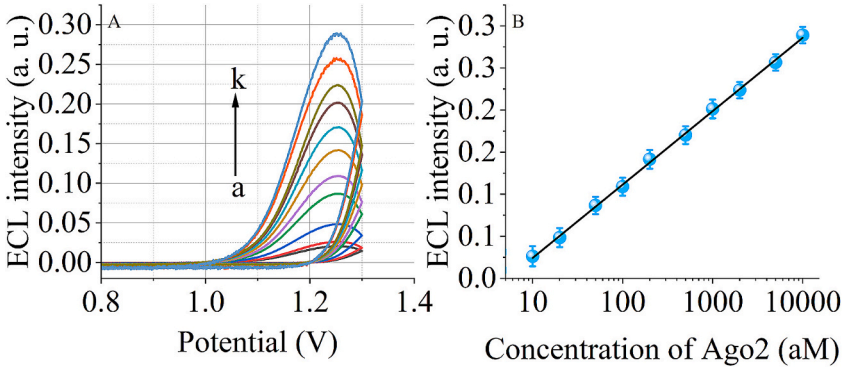


Fig. 3. (A) Electrochemiluminescence (ECL) response of the biosensor at varying concentrations of Ago2. (a to f) ECL intensity profiles obtained for Ago2 concentrations of 0, 10, 20, 50, 100, 200, 500, 1000, 2000, 5000, and 10,000 aM, respectively. The ECL signal increases with higher concentrations of Ago2, reaching a peak around 10 femtomolar (fM), indicating the optimal enzymatic cleavage by the DNA1-Ru conjugate for maximum signal generation. (B) A linear relationship between the logarithmic values of Ago2 concentrations and the corresponding ECL intensities is observed, described by the regression eq. $Y = -0.0629 + 0.0872\ \lg X$, with an R^2 value of 0.9990, confirming the precision of the biosensor in quantifying Ago2 levels.

each target DNA, resulting in a substantial increase in the electrochemiluminescence (ECL) signal. This second stage of amplification is particularly critical for boosting sensitivity, as Cas12a-mediated collateral cleavage can exponentially increase the signal output, making the system capable of detecting extremely low levels of Ago2 with high accuracy and specificity.

Together, these two amplification stages work synergistically. The HCR step increases the concentration of the target DNA, while the Cas12a cleavage step amplifies the signal at a much higher scale, ensuring that even trace amounts of Ago2 can be detected with remarkable precision. This multi-stage amplification strategy significantly improves the biosensor's overall performance, enabling detection of ultra-low biomarker concentrations in clinical diagnostic applications. The combination of HCR and Cas12a amplification, coupled with ECL as the readout mechanism, showcases the power of integrating different molecular strategies to achieve superior detection capabilities.

The biosensor's precision, sensitivity, and robustness make it especially valuable for applications that require reliable detection of trace biomarkers. Furthermore, the approach could be adapted for detecting a wide range of other biomolecules, highlighting the versatility and broad applicability of this biosensor design in various clinical and diagnostic contexts.

3.5. Specificity assay

To assess the selectivity of the newly developed biosensor, various Argonaute proteins, including Argonaute1 (Ago1) and Argonaute3 (Ago3), were tested as potential interferents under identical conditions. Fig. 4A demonstrates that the ECL signals for the control samples—each containing 10,000 aM of Ago1, Ago3, a mixture of Ago1, Ago2 and Ago3 (Mixture), or a blank—remained at consistently low levels, indicating minimal non-specific interactions. This observation confirms that the biosensor does not cross-react with these non-target analogs, thereby minimizing false-positive results. In stark contrast, the introduction of 10,000 aM of Ago2 led to a significant reduction in ECL intensity, clearly differentiating it from the control proteins. This pronounced drop in signal, which is consistent with the expected response for Ago2 alone, highlights the biosensor's high specificity and capability to accurately distinguish Ago2 from other Argonaute family members. Such specificity is critical in ensuring reliable detection, especially when dealing with complex biological samples that may contain structurally similar proteins or potential interferents.

Further evaluations were conducted to determine the reproducibility and stability of the biosensor. Fig. 4B illustrates the ECL intensity consistency across six independently fabricated biosensors, which showed minimal variation. The standard deviation (SD) was calculated to be approximately 0.00608, while the relative standard deviation (RSD) was around 2.17 %, signifying highly repeatable performance. Such reproducibility is crucial for practical applications where consistency between multiple biosensors is required for reliable data. In addition to reproducibility, the stability of the biosensor was also examined over time. As depicted in Fig. 4C, the biosensor retained 94.1 % of its original signal intensity after 14 days of storage under optimal conditions. This retention indicates excellent stability, suggesting that the biosensor is capable of maintaining its functional integrity over extended periods, thereby making it highly suitable for real-world diagnostic scenarios where storage stability is a key factor for usability and cost-effectiveness.

3.6. Real sample analysis

To evaluate the practical applicability of the developed biosensor, cell lysate samples were spiked with Ago2 at varying concentrations and subsequently diluted tenfold to simulate real-world sample conditions. Specifically, Ago2 was introduced at different concentrations (50 aM, 100 aM, 500 aM, and 1000 aM) into these diluted lysate samples. After spiking, the biosensor was used to measure the corresponding

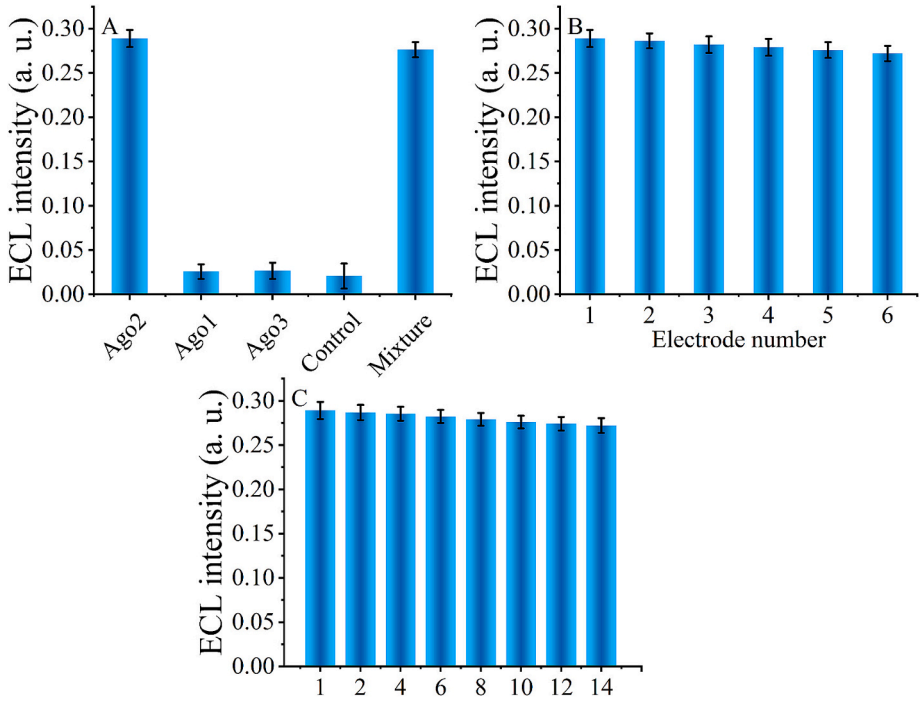


Fig. 4. Selectivity, Reproducibility, and Stability of the Biosensor. (A) Selectivity evaluation of the biosensor using 10,000 aM of different Argonaute proteins, including Ago1, Ago3, Ago2 and a mixture of Ago1, Ago2 and Ago3 (Mixture), as well as a blank control. The minimal ECL signals observed for Ago1, Ago3, and the blank indicate negligible non-specific interactions, whereas the significant reduction in ECL intensity in the presence of Ago2 demonstrates the biosensor's high specificity. (B) Reproducibility assessment of the biosensor across six independently fabricated devices. The minimal variation in ECL intensity (SD = 0.00608, RSD = 2.17 %) confirms the high repeatability of the biosensor's performance. (C) Stability analysis of the biosensor over a 14-day storage period. The biosensor retained 94.1 % of its original ECL signal under optimal storage conditions, highlighting its excellent long-term stability and suitability for real-world diagnostic applications.

electrochemiluminescence (ECL) signals for each concentration of Ago2. These signals were recorded and analyzed to assess the detection capabilities of the biosensor in complex biological environments. Using a standard linear calibration curve, the recorded ECL intensities were converted into Ago2 molar concentrations, which were then used to calculate the recovery rates of the biosensor in these matrices. The use of a standard calibration curve allowed for accurate conversion of ECL signals into quantitative values of Ago2, enabling an effective evaluation of the biosensor's recovery and detection accuracy.

The performance of the biosensor in these complex biological samples is summarized in Table 1. The results indicate that the biosensor exhibited high precision, as evidenced by the relative standard deviations (RSDs), which ranged from 2.56 % to 5.23 %, demonstrating minimal variability across repeated measurements. Furthermore, the calculated recovery rates for Ago2 detection ranged from 100.12 % to 102.97 %, illustrating the biosensor's high accuracy in quantifying the target analyte. These findings demonstrate that the biosensor is capable of delivering reliable detection in complex biological samples, reflecting its robustness and potential for practical applications. The ability to achieve such high precision and accuracy in the context of biological matrices underscores the biosensor's suitability for clinical diagnostics and biological research. Moreover, the consistency in recovery rates suggests that the biosensor could be used for quantitative analysis in real-world diagnostic scenarios, where analyzing complex biological matrices with high accuracy is critical.

3.7. Future directions and improvements

While the biosensor presented in this study demonstrates excellent sensitivity and specificity, further improvements are necessary to enhance its practical application. Future work could focus on optimizing the system for high-throughput screening by miniaturizing the assay and integrating it into automated platforms. Additionally, exploring the potential for multiplexed detection could broaden the range of applications, allowing simultaneous analysis of multiple biomarkers in a single sample. Improving the robustness of the biosensor, particularly in complex biological samples, will also be essential to ensure its reliability in real-world clinical settings.

Another area for future development involves increasing the cost-effectiveness and accessibility of the biosensor. Streamlining reagent synthesis and reducing the overall cost of materials would facilitate its adoption in resource-limited environments. Furthermore, adapting the biosensor for point-of-care applications by developing portable devices or mobile platforms could significantly enhance its utility in field diagnostics, providing rapid results outside of traditional laboratory settings. These advancements would greatly expand the impact of the biosensor in both clinical and research applications.

4. Conclusions

This study presents a novel electrochemiluminescence (ECL) biosensor that combines hybridization chain reaction (HCR) amplification and CRISPR/Cas12a technology for the highly sensitive and specific detection of Argonaute 2 (Ago2) activity. By leveraging Ago2's RNA cleavage specificity, HCR's non-enzymatic amplification capability, and Cas12a's collateral cleavage activity, the biosensor achieves a remarkable detection limit of 0.126 aM while maintaining excellent specificity and reproducibility. The system's multi-stage amplification approach significantly enhances signal output, enabling precise detection of Ago2 even in complex biological samples. The biosensor demonstrated robust performance in real-world conditions, accurately quantifying Ago2 in spiked cell lysates with recovery rates exceeding 100 %. Its stability, reproducibility, and adaptability to various sample types highlight its potential for clinical diagnostics, therapeutic monitoring, and early disease detection. Additionally, the integration of ECL as a signal output ensures low background noise and high sensitivity, making this platform highly practical for detecting trace biomarkers. Overall, this biosensor represents a significant advancement in molecular diagnostics, providing a versatile and efficient tool for the detection of low-abundance biomolecules. The proposed design can be further adapted for detecting other targets, underscoring its potential as a powerful platform for personalized medicine and next-generation diagnostic technologies.

Source of biological material

No biological materials from human or animal subjects were used in this study.

Statement on animal welfare

This research did not involve any animal experimentation. No animals were used in the research process, and animal welfare guidelines were not applicable.

CRediT authorship contribution statement

Qiang Tang: Writing – original draft. **Jiayi Zhang:** Validation. **Jialuo Pang:** Data curation. **Yingying Huang:** Data curation. **Ying Guan:** Formal analysis. **Yuanxun Gong:** Funding acquisition. **Qianli Tang:** Validation, Methodology, Investigation. **Kai Zhang:** Visualization, Validation, Resources. **Xianjiu Liao:** Writing – review & editing.

Ethics approval

This study did not involve human participants, human data, or animal subjects. Therefore, ethics approval or institutional review board approval is not applicable.

Funding

This work was supported by the National Natural Science Foundation of China (82160907).

Declaration of competing interest

The authors declare that they have no known competing financial interests or personal relationships that could have appeared to influence the work reported in this paper.

Acknowledgements

We gratefully acknowledge the financial support of the National Natural Science Foundation of China (82160907), the Natural Science Foundation of Guangxi Province (2025GXNSFHA069115), the State Key Laboratory of Analytical Chemistry for Life Science (SKLACLS2314), the Guangxi key laboratory of basic and translational research of Bone and joint Degenerative Disease(21-220-06-202205),the Key Laboratory of Biomedical Analytical Chemistry and Clinical Molecular Diagnosis of Baise (2022-38-05);the Baise Engineering Research Center for Bioanalytical Chemistry Application and Clinical Molecular Diagnosis (2021-22-09); the Key Laboratory of Bioanalytical Chemistry and Clinical Molecular Diagnosis of Youjiang Medical University for Nationalities(2021-56-02).

Appendix A. Supplementary data

Supplementary data to this article can be found online at https://doi.org/10.1016/j.bioelechem.2025.108975.

Data availability

Data will be made available on request.

7. References

[1] S. Jiang, X. Zhang, D.-L. Li, T.-T. Wang, F. Ma, C.-Y. Zhang, Construction of a gold nanoparticle-based single-molecule biosensor for simple and sensitive detection of Argonaute 2 activity, J. Mater. Chem. B 10 (29) (2022) 5594–5601, https://doi.org/10.1039/D2TB00802E.

[2] K. Zhang, Z. Fan, Y. Huang, M. Xie, J. Zhao, J. Wang, A well-designed gold nanoparticle based fluorescence probe for assay Argonaute2 and let-7a interaction in living cells, Sensors Actuators B Chem. 312 (2020) 128000, https://doi.org/10.1016/j.snb.2020.128000.

[3] X. Zhang, P. Graves, Y. Zeng, Overexpression of human Argonaute2 inhibits cell and tumor growth, Biochim. Biophys. Acta 1830 (3) (2013) 2553–2561, https://doi.org/10.1016/j.bbagen.2012.11.013.

[4] J. Winter, S. Diederichs, Argonaute-3 activates the let-7a passenger strand microRNA, RNA Biol. 10 (10) (2013) 1631–1643, https://doi.org/10.4161/rna.26424.

[5] M.F. Schmidt, O. Korb, C. Abell, MicroRNA-specific Argonaute 2 protein inhibitors, ACS Chem. Biol. 8 (10) (2013) 2122–2126, https://doi.org/10.1021/cb400246k.

[6] F. Li, M. Chen, X. Sun, X. Wang, P. Li, A novel graphene oxide-based fluorescence assay for RNA endonuclease activity of mammalian Argonaute2 protein, Sensors Actuators B Chem. 182 (2013) 156–160, https://doi.org/10.1016/j.snb.2013.02.113.

[7] D.G. Zisoulis, Z.S. Kai, R.K. Chang, A.E. Pasquinelli, Autoregulation of microRNA biogenesis by let-7 and Argonaute, Nature 486 (7404) (2012) 541–544, https://doi.org/10.1038/nature11134.

[8] N. Yang, Y. Cao, P. Han, X. Zhu, L. Sun, G. Li, Tools for investigation of the RNA endonuclease activity of mammalian Argonaute2 protein, Anal. Chem. 84 (5) (2012) 2492–2497, https://doi.org/10.1021/ac2032854.

[9] N.T. Schirle, I.J. MacRae, The crystal structure of human Argonaute2, Science 336 (6084) (2012) 1037–1040, https://doi.org/10.1126/science.1221551.

[10] F. Li, P. Li, L. Yang, B. Tang, Simple and sensitive fluorescence detection of the RNA endonuclease activity of mammalian argonaute2 protein based on an RNA molecular beacon, Chem. Commun. 48 (100) (2012) 12192–12194, https://doi.org/10.1039/C2CC36404B.

[11] X. Ke, Y. Ou, Y. Lin, T. Hu, Enhanced chemiluminescence imaging sensor for ultrasensitive detection of nucleic acids based on HCR-CRISPR/Cas12a, Biosens. Bioelectron. 212 (2022), https://doi.org/10.1016/j.bios.2022.114428.

[12] K.T. Kim, S. Angerani, N. Winssinger, A minimal hybridization chain reaction (HCR) system using peptide nucleic acids, Chem. Sci. 12 (23) (2021) 8218–8223, https://doi.org/10.1039/d1sc01269j.

[13] Jihua Wei, Jiayi Zhang, Wei Wang, Haidong Zhou, Huade Ma, Yuanxun Gong, Qianli Tang*, Kai Zhang*, Xianjiu Liao*, Precision miRNA profiling: Electrochemiluminescence powered by CRISPR-Cas13a and hybridization chain reaction [J], Analytica Chimica Acta 1307 (2024) 342641.

[14] J. Ye, W. Huang, X. Jia, H. Song, Y. Zhou, R. Yuan, et al., Short-stranded DNA segment-modulated LAMP/H+ as signal transducer to guide CHA-cooperated amplifiable electrochemical biosensing, Anal. Chim. Acta 1295 (2024) 342329, https://doi.org/10.1016/j.aca.2024.342329.

[15] G. Papadakis, A.K. Pantazis, N. Fikas, S. Chatziioannidou, V. Tsiakalou, K. Michaelidou, et al., Portable real-time colorimetric LAMP-device for rapid quantitative detection of nucleic acids in crude samples, Sci. Rep. 12 (1) (2022) 3775, https://doi.org/10.1038/s41598-022-06632-7.

[16] X. Zhao, Q. Han, N. Na, J. Ouyang, Spatiotemporally controlled DNA Nanoclamps: single-molecule imaging of receptor protein oligomerization, Anal. Chem. 93 (43) (2021) 14514–14520, https://doi.org/10.1021/acs.analchem.1c03282.

[17] X. Mi, H. Li, R. Tan, B. Feng, Y. Tu, The TDs/aptamer cTnI biosensors based on HCR and au/Ti3C2-MXene amplification for screening serious patient in COVID-19 pandemic, Biosens. Bioelectron. 192 (2021) 113482, https://doi.org/10.1016/j.bios.2021.113482.

[18] Y. Zou, H. Zhang, Z. Wang, Q. Liu, Y. Liu, A novel ECL method for histone acetyltransferases (HATs) activity analysis by integrating HCR signal amplification and ECL silver clusters, Talanta 198 (2019) 39–44, https://doi.org/10.1016/j.talanta.2019.01.083.

[19] D. Ren, C. Sun, Z. Huang, Z. Luo, C. Zhou, Y. Li, A novel FRET biosensor based on four-way branch migration HCR for Vibrio parahaemolyticus detection, Sens. and Actuators B-Chem. 296 (2019), https://doi.org/10.1016/j.snb.2019.05.054.

[20] Y. Tang, X.-L. Zhang, L.-J. Tang, R.-Q. Yu, J.-H. Jiang, In situ imaging of individual mRNA mutation in single cells using ligation-mediated branched hybridization chain reaction (ligation-bHCR), Anal. Chem. 89 (6) (2017) 3445–3451, https://doi.org/10.1021/acs.analchem.6b04312.

[21] K. Zhang, Y. Bao, C. Ou, G. Zhu, Y. Zhang, Binding-induced activation of CRISPR-Cas12a using PAM-engineered toehold switch and DNA tile architectures for enhanced detection of thrombin, Sensors Actuators B Chem. (2024) 136547, https://doi.org/10.1016/j.snb.2024.136547.

[22] J. Zhang, Z. Li, C. Guo, X. Guan, L. Avery, D. Banach, et al., Intrinsic RNA targeting triggers indiscriminate DNase activity of CRISPR-Cas12a, Angew. Chem. Int. Ed. Eng. 63 (20) (2024) e202403123, https://doi.org/10.1002/anie.202403123.

[23] J. Zhang, Z. Li, C. Guo, X. Guan, L. Avery, D. Banach, et al., Intrinsic RNA targeting triggers indiscriminate DNase activity of CRISPR-Cas12a, Angew. Chem. Int. Ed. 63 (20) (2024) e202403123, https://doi.org/10.1002/anie.202403123.

[24] Y. Yu, Q. Li, W. Shi, Y. Yang, H. He, J. Dai, et al., Programmable Aptasensor for regulating CRISPR/Cas12a activity, ACS Sens. 9 (1) (2024) 244–250, https://doi.org/10.1021/acssensors.3c01881.

[25] L. Xie, L. Ma, Q. Wu, C. Guo, X. Long, L. Liu, et al., Integrated CRISPR/Cas12a with terminal protection strategy for homogeneous protein assay, Sensors Actuators B Chem. 420 (2024) 136462, https://doi.org/10.1016/j.snb.2024.136462.

[26] R. Xia, N. Ouyang, T. Wang, Y. Zhuang, P. Miao, Electrochemical detection of glutathione based on accelerated CRISPR/Cas12a trans-cleavage with MnO2 nanosheets, Chem. Commun. 60 (15) (2024) 2034–2037, https://doi.org/10.1039/D3CC06186H.

[27] H. Pian, H. Wang, H. Wang, F. Tang, Z. Li, Capillarity-powered and CRISPR/Cas12a-responsive DNA hydrogel distance sensor for highly sensitive visual detection of HPV DNA, Biosens. Bioelectron. 264 (2024) 116657, https://doi.org/10.1016/j.bios.2024.116657.

[28] H. Pian, H. Wang, H. Wang, F. Tang, Z. Li, Capillarity-powered and CRISPR/Cas12a-responsive DNA hydrogel distance sensor for highly sensitive visual detection of HPV DNA, Biosens. Bioelectron. 264 (2024) 116657, https://doi.org/10.1016/j.bios.2024.116657.

[29] L. Ma, L. Xie, Q. Wu, L. Yang, Y. Zhou, Y. Cui, et al., Integrating CRISPR-Cas12a and rolling circle-amplified G-quadruplex for naked-eye fluorescent “off-on” detection of citrus Alternaria, Int. J. Biol. Macromol. 262 (2024) 129983, https://doi.org/10.1016/j.ijbiomac.2024.129983.

[30] Q. Luo, C. Zhang, X. Deng, D. Liu, X. Pan, Y. Gong, et al., A CRISPR-Cas12a-based electrochemical biosensor for the detection of microphthalmia-associated transcription factor, Microchim. Acta 191 (1) (2024) 73, https://doi.org/10.1007/s00604-023-06164-5.

[31] B. Liu, W. Lu, Y. Huang, X. Zhang, X. Yuan, A label-free electrochemical sensor for the detection of two kinds of targets based on CRISPR/Cas12a system, Sensors Actuators B Chem. 406 (2024) 135406, https://doi.org/10.1016/j.snb.2024.135406.

[32] T. Li, J. Wang, J. Fang, F. Chen, X. Wu, L. Wang, et al., A universal nucleic acid detection platform combing CRISPR/Cas12a and strand displacement amplification with multiple signal readout, Talanta 273 (2024) 125922, https://doi.org/10.1016/j.talanta.2024.125922.

[33] Y. Zhou, S. Xie, B. Liu, C. Wang, Y. Huang, X. Zhang, et al., Chemiluminescence sensor for miRNA-21 detection based on CRISPR-Cas12a and cation exchange reaction, Anal. Chem. 95 (6) (2023) 3332–3339, https://doi.org/10.1021/acs.analchem.2c04484.

[34] M. Liu, W. Ma, Y. Zhou, B. Liu, X. Zhang, S. Zhang, A label-free Photoelectrochemical biosensor based on CRISPR/Cas12a system responsive deoxyribonucleic acid hydrogel and “click” chemistry, ACS Sens. 7 (10) (2022) 3153–3160, https://doi.org/10.1021/acssensors.2c01636.

[35] P. Li, Y. Ye, Y. Li, Z. Xie, L. Ye, J. Huang, A MoS2 nanosheet-based CRISPR/Cas12a biosensor for efficient miRNA quantification for acute myocardial infarction, Biosens. Bioelectron. 251 (2024) 116129, https://doi.org/10.1016/j.bios.2024.116129.

[36] X. Lei, L. Ding, X. Yang, F. Xu, Y. Wu, S. Yu, PAIT effect: padlock activator inhibits the trans-cleavage activity of CRISPR/Cas12a, Biosens. Bioelectron. 263 (2024) 116607, https://doi.org/10.1016/j.bios.2024.116607.

[37] C. Wang, W. Ma, T. Jia, X. Zhang, X. Fan, Label-free SERS-colorimetry dual-mode biosensor based on CRISPR/Cas12a triggered G-quadruplex capped magnetic meso-porous silica microspheres, Sensors Actuators B Chem. 422 (2025) 136452, https://doi.org/10.1016/j.snb.2024.136452.

[38] Jihua Wei, Zichun Song, Jiuying Cui, Yuanxun Gong, Qianli Tang, Xinlei Song*, Entropy-driven assisted T7 RNA polymerase amplification-activated CRISPR/Cas13a activity for SARS-CoV-2 detection in human pharyngeal swabs and environment by an electrochemiluminescence biosensor [J], Journal of Hazardous Materials 452 (2023) 131268.

[39] J. Ni, H. Lin, W. Yang, Y. Liao, Q. Wang, F. Luo, et al., Homogeneous Electrochemiluminescence biosensor for the detection of RNase a activity and its inhibitor, Anal. Chem. 91 (22) (2019) 14751–14756, https://doi.org/10.1021/acs.analchem.9b04194.

[40] D. Zhang, F. Ma, J. Leng, C.-Y. Zhang, A dual signal amplification-assisted DNAzyme biosensor for ultrasensitive detection of Argonaute 2 activity, Chem. Commun. 54 (97) (2018) 13678–13681, https://doi.org/10.1039/C8CC08553F.

[41] K. Zhang, W. Huang, Y. Huang, H. Li, K. Wang, X. Zhu, et al., DNA tetrahedron based biosensor for Argonaute2 assay in single cells and human immunodeficiency virus Type-1 related ribonuclease H detection in vitro, Anal. Chem. 91 (11) (2019) 7086–7096, https://doi.org/10.1021/acs.analchem.9b00011.